Theoretical prediction of ion conductivity in solid state HfO_2*

Zhang Wei(张 炜)[a], Chen Wen-Zhou(陈文周)[b], Sun Jiu-Yu(孙久雨)[b], and Jiang Zhen-Yi(姜振益)[b]†

[a] School of Science, Xi'an University of Posts and Telecommunications, Xi'an 710121, China
[b] Institute of Modern Physics, Northwest University, Xi'an 710069, China

(Received 13 December 2011; revised manuscript received 26 August 2012)

A theoretical prediction of ion conductivity for solid state HfO_2 is carried out in analogy to ZrO_2 based on the density functional calculation. Geometric and electronic structures of pure bulks exhibit similarity for the two materials. Negative formation enthalpy and negative vacancy formation energy are found for YSH (yttria-stabilized hafnia) and YSZ (yttria-stabilized zirconia), suggesting the stability of both materials. Low activation energies (below 0.7 eV) of diffusion are found in both materials, and YSH's is a little higher than that of YSZ. In addition, for both HfO_2 and ZrO_2, the supercells with native oxygen vacancies are also studied. The so-called defect states are observed in the supercells with neutral and +1 charge native vacancy but not in the +2 charge one. It can give an explanation to the relatively lower activation energies of yttria-doped oxides and +2 charge vacancy supercells. A brief discussion is presented to explain the different YSH ion conductivities in the experiment and obtained by us, and we attribute this to the different ion vibrations at different temperatures.

Keywords: ion conduction, diffusion in solids, ionic crystals, density functional calculations

PACS: 66.10.Ed, 66.30.–h, 66.30.hd, 71.15.Mb **DOI:** 10.1088/1674-1056/22/1/016601

1. Introduction

Zirconia, a widely used ceramics material, has drawn much attention of both theoretical and experimental studies[1–10] for its special properties. When doped by some oxides, especially Y_2O_3, cubic phase ZrO_2 is stabilized at room temperature as the YSZ (yttria-stabilized zirconia) with oxygen vacancies forming. As a result, the ion diffusion can easily take place, which makes the doped zirconia a fast-ion conductor.[11]

However, Hf, which is in the same column as Zr in the periodic table, was ignored until wide investigations in recent ten years. HfO_2, which possesses a fluorite structure, the same as the cubic ZrO_2 at high temperature, is surprisingly similar to ZrO_2 in many physical and chemical properties.[12,13] Much attention has been paid to its nanoscaled or film structure in the existing applications and experiments of HfO_2.[14–19] However, it is reported by Guo[20] that one can hardly achieve significantly higher conductivity in the nanostructured ZrO_2, which reminds us to consider the conductivity in solid state HfO_2. Though the conductivity of nanoscaled or film HfO_2 is considerable high, how will it be in solid state HfO_2? By analogy to ZrO_2, it is natural to suppose that HfO_2 may show the same ion conductivity. Is this assumption correct? However, to our best knowledge, few theoretical investigations have focused on the ion conductivity of solid state HfO_2 with a comparison to ZrO_2. Trubelja and Stubican[21] have reported that the ion conductivity of HfO_2 is 1.5–2.2 times lower than that of ZrO_2. It is necessary to re-study this topic.

In the present work, we carry out a thermodynamic simulation of ion diffusion for both HfO_2 and ZrO_2 systems using density functional theory (DFT) calculation. The native oxygen vacancy and its diffusion are also considered to have a comparison with the doped oxides (YSZ and YSH). Formation energy, coupling with diffusion, and activation energy are discussed in detail. The difference between the previous experiment and the present work is discussed. It is found that the ion vibration influenced by temperature is responsible for the difference.

2. Computational method

All the DFT calculations were performed using the Vienna *ab initio* simulation package (VASP)[22,23] working in a plane-wave basis set. The electron–ion interaction was described using the projector augmented wave method[24,25] with plane waves up to the energies of 500 eV and 520 eV for ZrO_2 and HfO_2, respectively. The exchange–correlation functional proposed by Perdew–Burke–Ernzerhof (PBE)[26] was used, and the generalized gradient approximation (GGA) was applied.[27] The unit bulk cell shown in Fig. 1(a), containing 4 M (M = Hf, Zr) and 8 O, was selected in order to maintain the cubic symmetry and the periodic boundary condition. A fundamental structure with lattice constants ($a_f = a_0$, $b_f = a_0/\sqrt{2}$, $c_f = a_0/\sqrt{2}$) corresponding to the unit bulk cell was chosen. The 2×2×2 pure supercell shown in Fig. 1(b), containing 16 M and 32 O, was used to simulate the process of diffusion, where $a_s = 2a_0$, $b_s = \sqrt{2}a_0$, and $c_s = \sqrt{2}a_0$. The

*Project supported by the National Natural Science Foundation of China (Grant Nos. 10647008 and 50971099) and the Research Fund for the Doctoral Program of Higher Education, China (Grant No. 20096101110017).

†Corresponding author. E-mail: jiangzy@nwu.edu.cn

© 2013 Chinese Physical Society and IOP Publishing Ltd

Brillouin-zone sampling was performed on a dense k-point mesh of 9×9×9 points. However, for the other supercells discussed in this paper, we used 3×5×5 points in order to converge the total energy to within 10 meV.

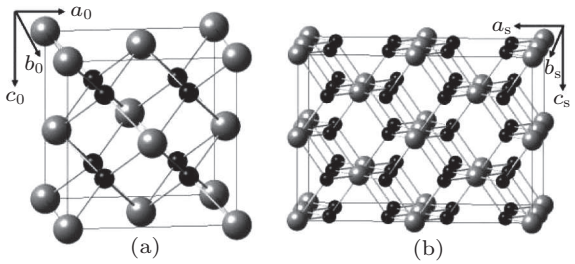


Fig. 1. Models of MO_2 (M=Hf, Zr) for (a) pure bulk and (b) supercell; small dark spheres represent O atoms; big gray spheres respresent M (M=Hf, Zr) atoms.

3. Pure HfO_2 & ZrO_2

The lattice of bulk is optimized to fit the Murnaghan equation of state. The total energy of each material as a function of volume is illustrated in Fig. 2. The calculated lattice constants and other structure information are also listed in Table 1, and the available results of the previous calculation and experimental studies[28,29] are also shown. The total density of states (DOS) is displayed in Fig. 3. It is obvious that HfO_2 and ZrO_2 have similar DOS structures, especially for the valence electrons. The band gaps (E_g) of HfO_2 and ZrO_2 are 3.8 eV and 3.2 eV, respectively. Though the calculated band gap of ZrO_2 is smaller than the experimental value (4.6 eV),[30] this underestimation is common in DFT simulations. All these similar results give us a primary understanding that pure MO_2 (M=Hf, Zr) has almost the same geometric and electronic behaviors.

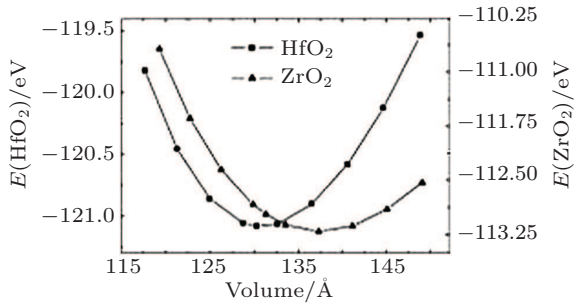


Fig. 2. Volume dependences of total energy for HfO_2 (left) and ZrO_2 (right).

Table 1. Lattice constants a_0 and bulk moduli B obtained in the present work, other calculation work, and experiments for MO_2 (M=Hf, Zr).

Reference	Method	a_0/Å	B/ GPa
HfO_2			
	exp.	5.08[a]	
Ref. [12]	LDA	5.26	280
Present	GGA	5.08	246.7
ZrO_2			
	exp.	5.09[b]	194–254[c]
Ref. [12]	LDA	5.07	267
Present	GGA	5.15	246.5

[a] Ref. [28], [b] Ref. [1], [c] Ref. [29]

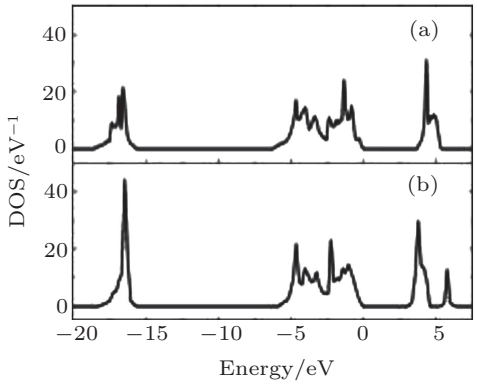


Fig. 3. Total densities of states (DOS) for pure (a) HfO_2 and (b) ZrO_2.

4. Native defects and diffusion

4.1. Stability

Before doping with yttrium, we consider the native oxygen vacancies and the oxygen ion diffusion in order to have a better understanding of the ion conduction mechanism. The oxygen atom at the fractional coordination of (0.375, 0.25, 0.5) is moved out to form an oxygen vacancy (expressed as V_O^q in the following). The supercells after moving out an O are set to carry 0, +1, and +2 charge and expressed as V_O, V_O^{1+}, and V_O^{2+}, respectively The ions occupying the first and the second nearest neighbor (NN) positions to V_O^q are allowed to relax in the calculation, while the others are fixed. The formation energy (E^F)[31–36] is defined as

$$E^F(V_O^q) = E_{tot}(M_nO_{2n-1}) - E_{tot}(M_nO_{2n}) + \mu_O + qE_F, \quad (1)$$

where $E_{tot}(M_nO_{2n-1})$ is the total energy of a supercell containing one oxygen vacancy in the charge state q, and $E_{tot}(M_nO_{2n})$ is the total energy of a MO_2 perfect crystal in the same supercell. The effect of removing one oxygen atom is expressed by its chemical potential μ_O, and we use the half energy of the oxygen molecule as the chemical potential of O. If the vacancy is charged, the formation energy depends further on the Fermi level (E_F), ranging from 0 to band gap (E_g) of MO_2, which is the energy of the reservoir for electrons.[37] We define E^F_{min} as the formation energy when $E_F = 0$, while E^F_{max} is considered when $E_F = E_g$. The calculated results for charged vacancies are given in Table 2. A similar trend found in another work[13] demonstrates that V_O^{2+} is more easily to form because of the smallest formation energy. In addition, the densities of states of all three supercells with vacancies are shown in Figs. 4 and 5 for HfO_2 and ZrO_2, respectively, which will be used in the further analysis.

Table 2. Maximum and minimum formation energies E^{F}_{max} and E^{F}_{min}, and activation energies E_a of ion diffusion for native defected MO_2 (M=Hf, Zr); maximum and minimum formation energies E^{F}_{max} and E^{F}_{min}, formation enthalpy ΔH, minimum activation energy E_a, and average activation energy among all the configurations for YSM (M=Hf, Zr). The quantities are given in units of eV.

		Native vacancy			YSM	
		0	+1	+2	Min.	Average
HfO_2	E^{F}_{max}	6.062	3.336	–0.492	3.954	4.029
	E^{F}_{min}		–0.554	–8.272	–5.016	–4.941
	ΔH				–0.23	–0.15
	E_a	1.657	0.749	0.435	0.503	0.550
ZrO_2	E^{F}_{max}	6.597	2.879	–0.818	2.264	2.484
	E^{F}_{min}		–0.271	–7.118	–6.706	–6.506
	ΔH				–0.25	–0.14
	E_a	1.213	0.702	0.424	0.495	0.536

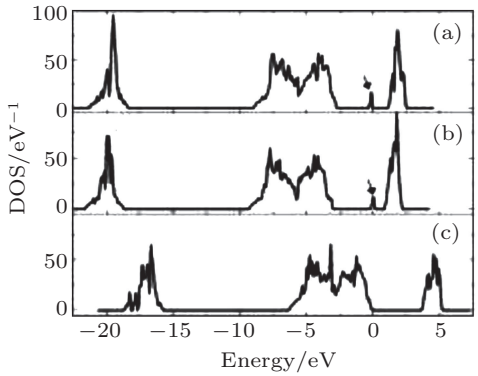


Fig. 4. Total densities of states (DOS) for native oxygen vacancy of HfO_2 with charge (a) 0, (b) +1, and (c) +2.

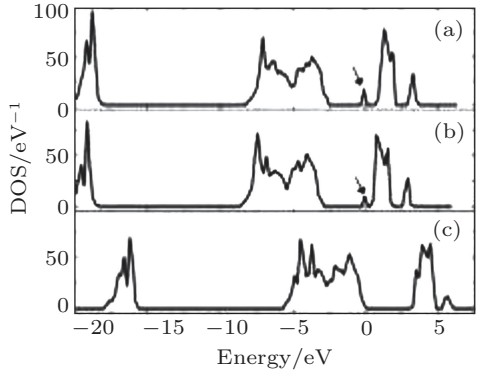


Fig. 5. Total densities of states (DOS) for native oxygen vacancy of ZrO_2 with charge (a) 0, (b) +1, and (c) +2.

4.2. Diffusion

To explore the ion diffusion, we consider one of the O ions nearest to the vacancy that migrates towards the vacancy. The static estimation of activation energy is performed by fixing the selected mobile O atom at several positions along the pathway. The total energies of these configurations are calculated to draw the potential energy surface of diffusion. The activation energy E_a is defined as the energy difference between the saddle point and the initial (or final) point of the potential surface along the pathway. We have selected different pathways for the O anion, such as along the directions of ⟨100⟩, ⟨110⟩, and ⟨111⟩. It turns out that the ⟨100⟩ direction (see sketch in the left of Fig. 6(a)) is the most possible pathway with a relatively smaller E_a, so the other pathways will not be discussed. In Table 2, we list the calculated values of E_a for supercells in different charge states. The HfO_2 and ZrO_2 have nearly the same activation energy, especially for V_O^{2+}, which are 0.435 eV and 0.424 eV, respectively. It is found that V_O^{2+} exhibites the smallest activation energy. The total energy as a function of the fractional coordination along the ⟨100⟩ direction is shown in Fig. 6(b).

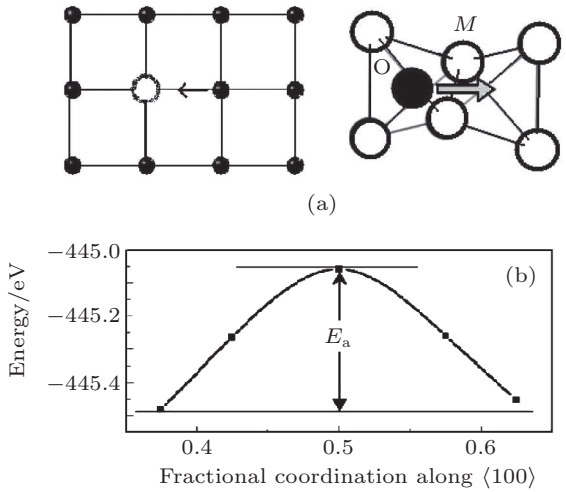


Fig. 6. (a) Left: sketch of diffusion pathway and direction along ⟨100⟩ for an oxygen ion, the ideal oxygen sublattice is shown. Black spheres are O atoms and the white sphere is an O vacancy. Right: sketch of the circumstance in which the O ion (black sphere) passes across the M–M (M=Hf, Zr; white sphere) edge of metal tetrahedron along the pathway. (b) Coordination dependence of total energy along the pathway for +2 charged supercell of native vacancy.

From the DOS figures, we find almost the same electronic structures for HfO_2 and ZrO_2. We can see that the most obvious difference between V_O^{2+} and V_O (or V_O^{1+}) for both two materials is the electronic occupation (pointed out by the arrows in figures) between the valence-band maximum (VBM) and the conduction-band minimum (CBM). It is the so-called defect state (or level), in which electrons are trapped around the vacancy and the charge density is relatively higher. When the O ion moves towards the vacancy, it will experience extra repulsion from the electrons in the defect state, making the activation energy larger. While in the V_O^{2+} supercell, no defect state is found in the DOS, which explains the smaller E_a than that of the former two supercells.

5. Y-doped oxides and diffusion

5.1. Model description

For Y doped oxides, in the supercell of each material, we substitute two Hf or Zr by Y. The oxygen atom at position (0.375, 0.25, 0.5), which is the position of the native

vacancy, is moved out to maintain the systems neutrality. Accordingly, the mol percentage of Y_2O_3 is about 6.7%, which is a little lower than the experimental value 8–40% in Ref. [38]. We have considered various relative vacancy positions and Y atoms in the doped structures. As reported in Refs. [3] and [5], in agreement with experiments, the Y ions prefer to occupy the 2nd NN position to V_O^q. In order to confirm it, we have simulated several different configurations: (i) two Y atoms in the 1st NN positions, (ii) one in the 1st NN position & one in the 2nd NN position, and (ii) two Y atoms in the 2nd NN positions to oxygen vacancy. Our results support the conclusion above, which enables us to exclude the configurations with Y ions in the 3rd NN positions to V_O^q. In this section, we allow all the atoms to relax in all the calculations to obtain better results. The total densities of states (DOS) of both YSH and YSZ are shown in Fig. 7 in order to compare with that of the native vacancy.

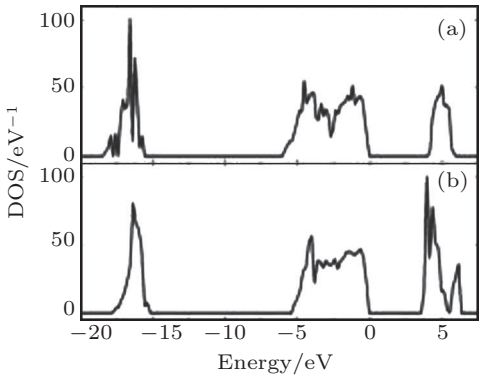


Fig. 7. Total densities of states (DOS) for (a) YSH and (b) YSZ.

5.2. Stability

The stabilities of YSH and YSZ are firstly assumed by the reaction

$$M_nO_{2n} + 2Y \rightarrow M_{n-2}Y_2O_{2n-1} + O + 2M, \tag{2}$$

and the formation energy is similar to that given in Eq. (1)

$$E^F = E_{tot}(M_{n-2}Y_2O_{2n-1}) - E_{tot}(M_nO_{2n}) + \mu_O + 2\mu_M - 2\mu_Y, \tag{3}$$

where μ_O adopts the same value used in the native vacancies. Chemical potential μ_M is calculated as the single atom energy in the M crystal. For μ_Y, the energy of yttrium ranging from -1.98 eV (free atom) to -6.47 eV (crystal) is considered. The minimum and the maximum of E^F (E^F_{min} and E^F_{max}) are listed in Table 2. It should be noted that we do not show E^F_{min} and E^F_{max} for all configurations. Instead, the quantities of configurations with the lowest total energy are picked out to display in the Min. column, and the Average column lists the average values of all configurations. Compared to those of V_O and V_O^{1+}, the formation energies (minimum) of YSM (M=Hf, Zr) and V_O^{2+} are more negative, ranging approximately from -5.0 eV to -8.2 eV, which indicates the stability of the oxygen vacancy in YSM.

We also use the formation enthalpy ΔH deduced from Ref. [4], which is defined as

$$\Delta H = E(M_{n-2}Y_2O_{2n-1}) - (n-2)E(MO_2) + E(Y_2O_3), \tag{4}$$

where x is the mol percentage of Y_2O_3. Here, we take the same method as described above to calculate the total energy of Y_2O_3. The unit cell of Y_2O_3 used here has a bixbyite structure containing 80 atoms. The lowest values of ΔH for all configurations of YSH and YSZ are listed in Table 2, which are about -0.23 eV and -0.25 eV, respectively. The negative ΔH demonstrates that the cubic MO_2 is stabilized by doping Y_2O_3.

5.3. Diffusion and conductivity

We select the same pathway and initial position for the mobile oxygen ion as those in the native vacancy. The O ion passes from the M–M (M=Hf, Zr) edge of metal tetrahedron along the pathway. The sketch is shown in the right of Fig. 6(a), where the gray spheres represent the M atoms. With the same method adopted for the native vacancy, we calculate the diffusion barrier E_a, as listed in Table 2. The data of E_a are processed under the same principle used for the formation energy E^F and shown in Min. and Average columns. Since the curves of the position dependence of total energy have similar trend with that of the native vacancy, we do not show them here. The minimum E_a for both materials is about 0.5 eV, which is not much lower than the average value. We then estimate the conductivity using the average value.

Since the oxygen ion is assumed to move on the anion sublattice by exchanging with the oxygen vacancy on the nearest neighbor site with a distance d, it is regarded as a hop. In this hopping process, the O ion passes across the M–M edge of metal tetrahedron along the $\langle 100 \rangle$ direction. Using the Boltzmann relationship and treating the process as Brownian movement, we finally obtain the ion conductivity

$$\sigma = (n_0 q^2 / k_B T) v_0 d^2 \exp(-E_a / k_B T), \tag{5}$$

where n_0 is the number of vacancies per unit volume. Since the other parameters are the same for YSH and YSZ, the values of ionic conductivity for both materials are of little difference for close E_a. Accordingly, at 1000 K, the ion conductivity will be 4.5 $\Omega^{-1}\cdot m^{-1}$ approximately, which is higher than that of many other ionic crystals.

For all the similar properties mentioned above, especially the high ion conductivity, it is reasonable to predict that HfO_2 (or YSH) can possibly behave as a fast-ion conductor such as ZrO_2 or YSZ.

5.4. Discussion

It is noted that there are several similar properties between V_O^{2+} and YSM (M=Hf, Zr), including the number of electrons, DOS, and activation energy. Obviously, there is no defect state found in the figures of DOS. This means that the diffusion barrier is much weaker without the repulsion from electrons trapped around the vacancy. As a result, V_O^{2+} and YSM have similar activation energies, though E_a of YSM is a little higher because of the stronger repulsion from the Y ions than that from the Zr ions, which is due to the larger radius of Y ions.

We only consider the situation that the O ion passes across the M–M (M=Hf, Zr) edge rather than M–Y and Y–Y edges, because it is reported in Ref. [10] that the M–M edge is much more easy for the O ion to pass compared to M–Y and Y–Y edges. In addition, if the mobile O ion takes the other two pathways, there must be a Y ion in the 1st NN postion to V_O^q, which is not likely to be stable in thermodynamics.[4,5] It is confirmed again in the present work by calculating the YSM supercell with two Y ions in the1st NN positions to V_O^q. The formation energy is −6.0 eV, which is larger than that of the lowest E^F supercell presented above. In addition, for both YSH and YSZ, when O moves across the Y–Y edge, the calculated barriers are around 1.1 eV, which is as large as that in YSZ presented in Ref. [10]. Hence, the probability for the O ion to pass across M–Y and Y–Y edges is much smaller, which can be ignored.

The ion conductivity estimated by us also needs to be analyzed and discussed. Molecular dynamics simulations of YSZ have been performed by authors in Refs. [6]–[9], and only the exact values of conductivity are found in Ref. [6]. The conductivities at 1759 K presented in Ref. [6] (0.7 $\Omega^{-1}\cdot cm^{-1}$) and obtained in the present work (0.37 $\Omega^{-1}\cdot cm^{-1}$) match the experimental value (0.9 $\Omega^{-1}\cdot cm^{-1}$)[39] in the same order of magnitude. The difference in temperature is responsible for the different conductivities of our calculation and the experiment. Since the activation energy decreases with the increasing temperature, it is normal that the conductivity computed by us is lower than that obtained at the high temperature experiment, as the DFT simulation is performed at 0 K.

The ion conductivity of HfO_2 obtained in experiment[21] is 1.5–2.2 times lower than that of ZrO_2. The difference of ionic conductivity of YZH may be attributed to the following reasons. The jumps of O ions require a relative large space. Since the Hf ion is heavier (in mass) than the Zr ion, the Hf ion vibrates with smaller displacements. This leads to a lower probability to create suitable spaces for mobile O ions. The influence from the ion mass decreases as the temperature goes higher than 1000 K in the experiment. At higher temperatures, like 1500 K or even higher, the vibration states of Hf and Zr ions are similar, then YSH and YSZ should show similar ionic conductivity. However, in our quasi-static simulation, Hf and Zr ions show not much difference in diffusion process, resulting in similar conductivities. Thus, our prediction fits the situation at higher temperature.

6. Conclusion

A theoretical study of ion conductivity of solid state HfO_2 has been performed in analogy to ZrO_2. The geometric and the electronic structures show similar properties for both systems. In all supercells of HfO_2 and ZrO_2, yttria-doped oxides and +2 charge vacancies are most stable with the most negative formation energies. The diffusion of native oxygen vacancy and the yttrium doped models of HfO_2 and ZrO_2 have been studied by quasi-static simulations. Similar activation energies are found in YSH and YSZ, resulting in the similarity of ionic conductivity. The ion conductivity estimated is in agreement with the experimental value for YSZ. In addition, the native vacancy model with +2 charge has relatively low activation energies as YSZ and YSH, whose diffusion mechanism can be primarily explained by the electronic distribution from DOS. A lower ion conductivity of YSH than that of YSZ is reported in experiment, we explain that different vibrations of Hf and Zr cations at different temperatures are responsible for the difference. Accordingly, we predict that at high temperature, HfO_2 will show higher ionic conductivity and could possibly be a fast-ion conductor.

References

[1] Aldebert P and Traverse J 1985 *J. Am. Ceram. Soc.* **68** 34
[2] Zhao X, Ceresoli D and Vanderbilt D 2005 *Phys. Rev.* B **71** 085107
[3] Stapper G, Bernasconi M, Nicoloso N and Parrinello M 1999 *Phys. Rev.* B **59** 797
[4] Bogicevic A, Wolverton C, Crosbie G M and Stechel E B 2001 *Phys. Rev.* B **64** 014106
[5] Ostanin S, Salamatov E, Craven A J, McComb D W and Vlachos D 2002 *Phys. Rev.* B **66** 132105
[6] Perumal T P, Sridhar V, Murthy K P N, Easwarakumar K S and Ramasamy S 2002 *Physica* A **309** 35
[7] Pornprasertsuk R, Ramanarayanan P, Musgrave C B and Prinz F B 2005 *J. Appl. Phys.* **98** 103513
[8] Krishnamurthy R, Yoon Y G, Srolovitz D J and Car R 2004 *J. Am. Ceram. Soc.* **87** 1821
[9] Krishnamurthy R, Srolovitz D J, Kudin K N and Car R 2005 *J. Am. Ceram. Soc.* **88** 2143
[10] Pietrucci F, Bernasconi M, Laio A and Parrinello M 2008 *Phys. Rev.* B **78** 094301
[11] Wagner C 1943 *Naturwissenschaften* **31** 265
[12] Lowther J E, Dewhurst J K, Leger J M and Haines J 1999 *Phys. Rev.* B **60** 14485
[13] Zheng J X, Ceder G, Maxisch T, Chim W K and Choi W K 2007 *Phys. Rev.* B **75** 104112
[14] Fiorentini V and Gulleri G 2002 *Phys. Rev. Lett.* **89** 266101
[15] Ramo D M Shluger A L, Gavartin J L and Bersuker G 2007 *Phys. Rev. Lett.* **99** 155504
[16] Tang C, Tuttle B and Ramprasad R 2007 *Phys. Rev.* B **76** 073306
[17] Cho D Y, Jung H S and Hwang C S 2010 *Phys. Rev.* B **82** 094104
[18] Robertson J, Sharia O and Demkov A A 2007 *Appl. Phys. Lett.* **91** 132912

[19] Smirnova T P, Yakovkina L V, Beloshapkin S A, Kaichev V V, Alferova N I and Song J H 2010 *J. Phys. Chem. Solids* **71** 836
[20] Guo X 2011 *Scr Mater.* **65** 96
[21] Trubelja M F and Stubican V S 1991 *Solid State Ionics* **49** 89
[22] Kresse G and Hafner J 1993 *Phys. Rev.* B **47** 558
[23] Kresse G and Furthmuller J 1996 *Phys. Rev.* B **54** 11169
[24] Blochl P E 1994 *Phys. Rev.* B **50** 17953
[25] Kresse G and Joubert D 1998 *Phys. Rev.* B **59** 1758
[26] Perdew J P, Burke K and Ernzerhof M 1996 *Phys. Rev. Lett.* **77** 3865
[27] Perdew J P, Chevary J A, Vosko S H, Jackson K A, Pederson M R, Singh D J and Fiolhais C 1992 *Phys. Rev.* B **46** 6671
[28] Stacy D W, Johnstone J K and Wilder D R 1972 *J. Am. Ceram. Soc.* **55** 482
[29] Ingel R P and Lewis D 1988 *J. Am. Ceram. Soc.* **71** 265
[30] McComb D W 1996 *Phys. Rev.* B **54** 7094
[31] Ye H G, Chen G D, Zhu Y Z and Lü H M 2007 *Chin. Phys.* **16** 3803
[32] Fang Z J, Shi L J and Liu Y H 2008 *Chin. Phys.* B **17** 4279
[33] Wang K P and Huang Y 2011 *Chin. Phys.* B **20** 077401
[34] Zhang J, Liang E J, Sun Q and Jia Y 2012 *Chin. Phys.* B **21** 047201
[35] Zhang L Y, Yan J L, Zhang Y J and Li T 2012 *Chin. Phys.* B **21** 067102
[36] Qiao Z J, Chen G D, Ye H G, Wu Y L, Niu H B and Zhu Y Z 2012 *Chin. Phys.* B **21** 087101
[37] Janotti A and Van de Walle C G 2006 *J. Cryst. Growth* **287** 58
[38] Pascual C and Duran P 1983 *J. Am. Ceram. Soc.* **66** 22
[39] Murch G E 1982 *Solid State Ionics* **7** 177